EXPONENTIAL REACHING LAW-BASED SLIDING MODE CONTROL FOR A 2-DOF PLANAR ROBOT: ROBUSTNESS TO DISTURBANCES AND MASS VARIATIONS

BỘ ĐIỀU KHIỂN TRƯỢT DỰA TRÊN LUẬT HÀM MŨ CHO ROBOT NỐI TIẾP HAI BẬC TỰ DO: BỀN VỮNG VỚI NHIỄU VÀ THAY ĐỔI THAM SỐ

Van Vuong Dinh

Electric Power University, Hanoi, Viet Nam
Ngày nhận bài: 12/05/2025, Ngày chấp nhận đăng: 08/7/2025

Abstract:

This paper presents a robust sliding mode control (SMC) strategy based on an exponential reaching law for a two-degrees-of-freedom (2-DoF) planar robotic manipulator. The proposed controller is designed to achieve fast and accurate convergence of tracking errors while mitigating the chattering effects typically associated with conventional SMC approaches. By incorporating an exponentially decaying term into the reaching law, the controller enhances the smoothness of the sliding motion and improves the transient performance of the system. The dynamic model of the robotic manipulator is derived using the Euler–Lagrange formulation to capture the system's nonlinear and coupled dynamics. A Lyapunov-based stability analysis is employed to establish the asymptotic stability of the closed-loop system. To evaluate the controller's effectiveness, extensive simulation studies are conducted under various scenarios, including nominal conditions, the presence of external disturbances, and significant variations in link mass parameters. The simulation results confirm excellent trajectory tracking performance and strong robustness, thereby demonstrating the controller's adaptability to both ideal and uncertain environments. These results underline the potential of the proposed control scheme for practical applications in advanced robotic systems.

Keywords:

Exponential Reaching Law, Sliding Mode Control, 2-DoF Planar Robot, Trajectory Tracking, Robust Control.

Tóm tắt:

Bài báo này trình bày một chiến lược điều khiển trượt (SMC) bền vững, dựa trên luật tiếp cận hàm mũ, áp dụng cho cánh tay robot phẳng hai bậc tự do (2-DoF). Bộ điều khiển được đề xuất nhằm đảm bảo khả năng hội tụ nhanh và chính xác của sai số bám quỹ đạo, đồng thời giảm thiểu hiện tượng rung (chattering) vốn thường gặp trong các phương pháp SMC truyền thống. Việc tích hợp thành phần hàm mũ suy giảm vào luật tiếp cận giúp cải thiện độ mượt của chuyển động trượt và nâng cao đáp ứng quá độ của hệ thống. Mô hình động học của robot được xây dựng dựa trên phương pháp Euler–Lagrange nhằm phản ánh chính xác các đặc tính phi tuyến và tương tác giữa các khớp. Phân tích ổn định dựa trên lý thuyết Lyapunov được sử dụng để chứng minh tính ổn định tiệm cận của hệ thống kín. Các nghiên cứu mô phỏng được thực hiện trong nhiều điều kiện khác nhau, bao gồm điều kiện định mức, có nhiễu ngoài, và sai lệch lớn về thông số khối lượng của các khâu. Kết quả cho thấy bộ điều khiển đạt hiệu năng bám quỹ đạo cao và độ bền vững mạnh mẽ, khẳng định tính hiệu quả và khả năng thích ứng của phương pháp đề xuất trong cả môi trường lý tưởng và bất định.

Từ khóa:

Luật tiếp cận hàm mũ, Điều khiển trượt, Robot nối tiếp hai bậc tự do, Bám quỹ đạo, Điều khiển bền vững.

1. INTRODUCTION

The precise control of robotic manipulators remains a fundamental challenge in modern automation systems [1], [2], [3]. In both academic research and industrial applications, manipulators are expected to execute complex tasks with high precision, rapid response, and strong robustness against environmental uncertainties. Among various configurations, the two-degrees-of-freedom (2-DoF) planar robotic manipulator has been extensively investigated due to its nonlinear, coupled dynamics and its ability to represent the core behaviors of more complex robotic systems [4], [5], [6], [7]. Controlling such nonlinear systems demands advanced methodologies capable of guaranteeing both stability and performance in the presence of model uncertainties, external disturbances, and parameter variations.

Over the past few decades, various nonlinear control strategies have been applied to robotic manipulators, including feedback linearization, adaptive control, backstepping, and fuzzy logic control. Among these approaches, Sliding Mode Control (SMC) has attracted significant attention due to its inherent robustness and its capability to handle model uncertainties without requiring precise system knowledge [8], [9], [10]. The core concept of SMC is to steer the system trajectories toward a predefined sliding surface and maintain their motion along this surface, thereby ensuring convergence to the desired trajectory. Once the sliding condition is met, the system dynamics reduce to a lower-order, stable form that is highly resistant to certain classes of disturbances and parameter variations.

Despite its advantages, classical Sliding Mode Control (SMC) methods suffer from a significant drawback: chattering. This undesirable phenomenon results from the use of discontinuous control signals (e.g., the sign function), which can induce high-frequency oscillations, cause excessive wear on mechanical actuators, and even lead to instability in systems with unmodeled high-frequency dynamics. To mitigate chattering while preserving robustness, numerous strategies have been proposed, including boundary layer techniques, high-order SMC [11], fuzzy-tuned SMC [12], and modifications to the reaching law.

One promising approach to mitigate chattering is the implementation of an Exponential Reaching Law (ERL), which incorporates a decaying exponential term into the switching component of the control law [13], [14]. The ERL facilitates rapid convergence during the initial phase of motion and progressively decreases the switching effort as the system nears the sliding manifold. This adaptive behavior effectively reduces steady-state chattering without compromising the reaching performance, making ERL a highly practical and robust solution for practical control applications.

In this study, an Exponential Reaching Law-based Sliding Mode Controller (ERL-SMC) is designed and implemented for a two-degrees-of-freedom (2-DoF) planar robotic manipulator. The controller is developed using a model-based approach and ensures the asymptotic convergence of tracking errors through a rigorous Lyapunov stability analysis. The exponential reaching law incorporated into the control design introduces a time-decaying term that enhances transient response while reducing control effort as the system approaches steady-state.

To validate the effectiveness of the

proposed method, extensive simulation studies are conducted under a variety of operating scenarios. These include ideal tracking without disturbances, tracking in the presence of bounded external disturbances, and conditions with varying link masses to emulate modeling uncertainties. In all cases, the ERL-SMC exhibits excellent tracking accuracy and strong robustness, consistently maintaining system stability while effectively suppressing chattering.

The main contributions of this paper are as follows:

+ A sliding mode control strategy using an exponential reaching law tailored for nonlinear robotic manipulators.

+ A comprehensive stability proof using Lyapunov theory to guarantee global asymptotic stability of the closed-loop system.

+ Simulation-based validation under both nominal and challenging conditions, including external disturbances and significant mass variations.

The rest of the paper is organized as follows: Section 2 presents the dynamic modeling of the 2-DoF planar robot. Section 3 details the controller design and stability analysis. Section 4 discusses simulation results that illustrate the robustness and tracking performance of the proposed controller. Finally, Section 5 concludes the paper and suggests directions for future research.

2. MATHEMATICAL MODELING OF 2-DOF PLANAR ROBOT MANIPULATOR

This section presents the detailed mathematical model of the two-degrees-of-freedom (2-DoF) planar robotic manipulator used in this study. The 2-DoF planar robot manipulator considered in this study consists of two rigid links connected by revolute joints. The motion of the robot is confined to a horizontal plane, and the dynamic model is derived using the Euler-Lagrange formulation, which takes into account both the kinetic and potential energy of the system.

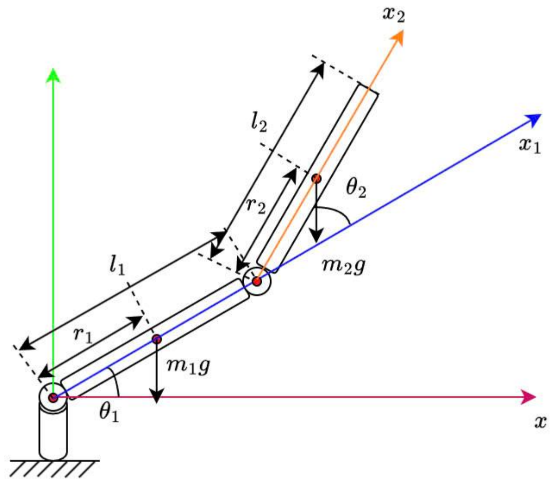

Figure 1. Schematic diagram of the 2-DoF planar robotic manipulator.

2.1. Kinematics and Generalized Coordinates

The schematic diagram of the robot is shown in Figure 1. Let θ_1 and θ_2 denote the angular positions of the first and second links, respectively. The generalized coordinate vector is defined as :

$$q = \begin{bmatrix} \theta_1 \\ \theta_2 \end{bmatrix} \quad (1)$$

Each link has the following parameters :

l_1, l_2 : lengths of link 1 and 2.

m_1, m_2 : masses of link 1 and 2.

I_1, I_2 : moments of inertia about the center of mass.

r_1, r_2 : distances from the joint to the center of mass of each link.

The forces acting on the system include gravitational forces m_1g and m_2g. Although the configuration is restricted to a horizontal plane, gravitational effects still influence the joint torques as a function of the angular positions.

2.2. Dynamic Model Using Lagrangian Approach

The dynamics of the robot are derived using the Euler-Lagrange method, which is based on the difference between the kinetic and potential energy of the system. The Lagrangian is given by: The Lagrangian $\mathcal{L}$ is defined as:

$$\mathcal{L} = \mathcal{T} - \mathcal{V} \quad (2)$$

where $\mathcal{T}$ is the total kinetic energy and $\mathcal{V}$ is the total potential energy.

Using the Euler-Lagrange equation, the equations of motion are expressed as:

$$\frac{d}{dt}\left(\frac{\partial \mathcal{L}}{\partial \dot{q}_i}\right) - \frac{\partial \mathcal{L}}{\partial q_i} = \tau_i, \quad i=1, \quad 2 \quad (3)$$

where τ_1 and τ_2 are the torques applied at the joints. The system dynamics can be expressed in matrix form as :

$$M(q)\ddot{q} + C(q,\dot{q})\dot{q} + G(q) = \tau \quad (4)$$

where:

$M(q) \in \mathbb{R}^{2\times 2}$: inertia matrix.

$C(q,\dot{q}) \in \mathbb{R}^{2\times 2}$: coriolis and centrifugal terms.

$G(q) \in \mathbb{R}^{2\times 1}$: gravity vector.

$\tau \in \mathbb{R}^{2\times 1}$: vector of control torques.

2.3. Explicit Expressions with Parameters

The inertia matrix $M(q)$, coriolis matrix $C(q)$, and gravity vector $G(q)$ are derived as follows:

$$M(q) = \begin{bmatrix} a_1 + 2a_2\cos(\theta_2) & a_3 + a_2\cos(\theta_2) \\ a_3 + a_2\cos(\theta_2) & a_3 \end{bmatrix} \quad (5)$$

$$C(q,\dot{q}) = \begin{bmatrix} -b_1\sin(\theta_2)\,\dot{\theta}_2 & -b_1\sin(\theta_2)\left(\dot{\theta}_1 + \dot{\theta}_2\right) \\ b_1\sin(\theta_2)\,\dot{\theta}_1 & 0 \end{bmatrix} \quad (6)$$

$$G(q) = \begin{bmatrix} g_1\cos(\theta_1) + g_2\cos(\theta_1+\theta_2) \\ g_2\cos(\theta_1+\theta_2) \end{bmatrix} \quad (7)$$

These expressions capture the nonlinear coupling and dynamic behavior of the robotic system. The coefficients in the corresponding matrices depend on the physical parameters of the manipulator, as detailed below. The parameters $a_1, a_2, a_3, b_1, g_1, g_2$ are defined as:

$$\begin{aligned} a_1 &= l_1 + l_2 + m_1 r_1^2 + m_2\left(l_1^2 + r_1^2\right) \\ a_2 &= m_2 l_1 r_2 \\ a_3 &= l_2 + m_2 r_2^2 \\ b_1 &= m_2 l_1 r \\ g_1 &= m_1 g r_1 + m_2 g l_1 \\ g_2 &= m_2 g r_2 \end{aligned} \quad (8)$$

Here, g denotes the gravitational acceleration. These parameters encapsulate both the mass and geometric properties of the manipulator.

3. CONTROLLER DESIGN USING EXPONENTIAL REACHING LAW-BASED SLIDING MODE CONTROL

This section presents the formulation of a robust sliding mode control (SMC) strategy, augmented by an exponential reaching law (ERL), for a two-degrees-of-freedom (2-DoF) planar robotic manipulator. The primary control objective is to ensure accurate tracking of predefined joint reference trajectories under a range of operating conditions, including model uncertainties, parameter variations, and external disturbances. Although conventional SMC guarantees robustness and finite-time convergence, it typically suffers from chattering effects caused by discontinuous control actions. To address this limitation, the proposed exponential reaching law introduces a smoother convergence mechanism, thereby reducing chattering while preserving robustness.

3.1. Tracking Error and Sliding Surface

To formulate the control law, we first define the trajectory tracking error as:

$$e(t) = q(t) - q_d(t) \quad (9)$$

$$\dot{e}(t) = \dot{q}(t) - \dot{q}_d(t) \quad (10)$$

where $q(t) \in \mathbb{R}^2$ is the actual joint position vector, and $q_d(t) \in \mathbb{R}^2$ is the desired trajectory vector. These quantities are assumed to be continuously differentiable.

The sliding surface $s(t)$ is subsequently constructed to encapsulate both the position and velocity tracking errors:

$$s(t) = \dot{e}(t) + \Lambda e(t) \quad (11)$$

where $\Lambda = diag(\lambda_1, \lambda_2)$ is a positive definite diagonal matrix, with its elements selected to achieve a desirable dynamic response. The purpose of this sliding surface is to enforce error dynamics that converge exponentially to zero when the system operates in sliding mode.

3.2. Exponential Reaching Law

The reaching phase plays a critical role in sliding mode control (SMC), as it determines how the system states converge to the sliding surface. Traditional reaching laws typically employ a discontinuous sign function, which often induces undesirable chattering. To enhance system performance and reduce chattering effects, an exponential reaching law is adopted in this study:

$$\dot{s}(t) = -ks(t) - \alpha sign\big(s(t)\big) + \beta e^{-\gamma t} sign(s(t)) \quad (12)$$

here:

+ $k > 0$ is a linear feedback gain promoting proportional decay.

+ $\alpha > 0$ sets the magnitude of the discontinuous term for robustness.

+ $\beta > 0$ and $\gamma > 0$ define the exponential modulation term.

The advantage of this reaching law lies in its dynamic adaptability: it applies strong corrective action during the early stage of error evolution and gradually reduces switching intensity as the system stabilizes. This approach preserves robustness while minimizing chattering, which is highly desirable for practical implementation in robotic systems.

3.3. Control Law Derivation

The dynamic model of the 2-DoF manipulator is written as:

$$M(q)\ddot{q} + C(q,\dot{q})\dot{q} + G(q) = \tau + d \quad (13)$$

where $M(q)$ is the inertia matrix, $C(q,\dot{q})$ accounts for Coriolis and centrifugal effects, $G(q)$ is the gravity vector, and $\tau \in \mathbb{R}^2$ is the control torque vector and d is the bounded external disturbance.

To ensure that the sliding surface dynamics obey the exponential reaching law, we design the control input τ as:

$$\tau = \tau_{eq} + \tau_{sw} \quad (14)$$

The equivalent control τ_{eq} compensates for the known nominal dynamics of the system:

$$\tau_{eq} = M(q)(\ddot{q}_d - \Lambda\dot{e}) + C(q,\dot{q})\dot{q} + G(q) \quad (15)$$

The switching control component τ_{sw} imposes the exponential reaching behavior:

$$\tau_{sw} = M(q)(-ks - \alpha sign(s) + \beta e^{-\gamma t} sign(s)) \quad (16)$$

Thus, the total control law becomes:

$$\tau = M(q)\big(\ddot{q}_d - \Lambda\dot{e} - ks - \alpha sign(s) + \beta e^{-\gamma t} sign(s)\big) + C(q,\dot{q})\dot{q} + G(q) \quad (17)$$

This structure ensures that the robot follows the reference trajectory with robustness and reduced chattering, even in the presence of unmodeled dynamics or parameter variations such as changes in link mass.

3.4. Stability Analysis

To analyze the stability of the closed-loop system, we consider the Lyapunov candidate function:

$$V(s) = \frac{1}{2} s^T s \quad (18)$$

Taking the time derivative:

$$\dot{V}(s) = s^T \dot{s} \quad (19)$$

$$= -k\|s\|^2 - \alpha\|s\|_1 + \beta e^{-\gamma t}\|s\|_1 \quad (20)$$

It is evident that:

+ The term $-k\|s\|^2$ ensures quadratic decay.
+ The term $-\alpha\|s\|_1$ ensures robustness via the sign function.
+ The final term $\beta e^{-\gamma t}\|s\|_1$ is bounded and vanishes as $t \to \infty$.

By choosing $\alpha > \beta$, we guarantee that:

$$\dot{V}(s) < 0 \quad \forall s \neq 0 \quad (21)$$

This implies that the system is globally asymptotically stable. As the sliding surface converges to zero, both the position and velocity tracking errors asymptotically converge to zero as well. The control structure for the proposed method is presented in Figure 2.

The proposed exponential reaching law-based sliding mode control (ERL-SMC) framework combines the robustness of classical SMC with enhanced convergence characteristics and mitigated switching effects. The control law is designed to compensate for the known system dynamics while maintaining robustness against model uncertainties and external disturbances. Theoretical analysis confirms the global asymptotic stability of the closed-loop system, which will be further validated through simulation results presented in the following section.

4. SIMULATION RESULTS

To evaluate the effectiveness of the proposed exponential reaching law-based sliding mode control (ERL-SMC), simulation studies were conducted using a two-degrees-of-freedom (2-DoF) planar robotic manipulator model. The controller was implemented in MATLAB/Simulink as seen in Figure 2, and its performance was assessed in terms of trajectory tracking accuracy, robustness to external disturbances, and resilience to model uncertainties such as mass variations.

The physical parameters of the robot are as follows: the mass of link 1 is $m_1 = 5.25\ kg$ and that of link 2 is $m_2 = 3.00\ kg$. Both links have a length of $l_1 = l_2 = 0.3\ m$. The gravitational acceleration is set to $g = 9.81\ m/s^2$. These values were used to derive the robot's dynamic model matrices, including the inertia matrix, Coriolis matrix, and gravity vector.

The desired end-effector trajectory is a circular path in the horizontal plane, defined in Cartesian space by:

$$x_d(t) = 0.3 + 0.1\cos(ft) \quad (22)$$

$$y_d(t) = 0.3 + 0.1\sin(ft) \quad (23)$$

$$\dot{x}_d(t) = -0.1f\sin(ft) \quad (24)$$

$$\dot{y}_d(t) = 0.1f\cos(ft) \quad (25)$$

This trajectory describes a circle of radius 0.1 m centered at position (0.3, 0.3) meters. The parameter f represents the angular frequency of motion and was selected to control the speed of the desired path.

For controller implementation, the desired position and velocity in Cartesian space were mapped into joint space using inverse kinematics and Jacobian-based velocity transformations.

The initial conditions of the robot were intentionally chosen to deviate from the reference trajectory of the controller. The initial joint angles were set to $\theta_1(0) = \frac{\pi}{3}$ and $\theta_2(0) = -\frac{\pi}{3}$, while the initial joint velocities were $\dot{\theta}_1(0) = 0$ and $\dot{\theta}_2(0) = 0.2$ rad/s.

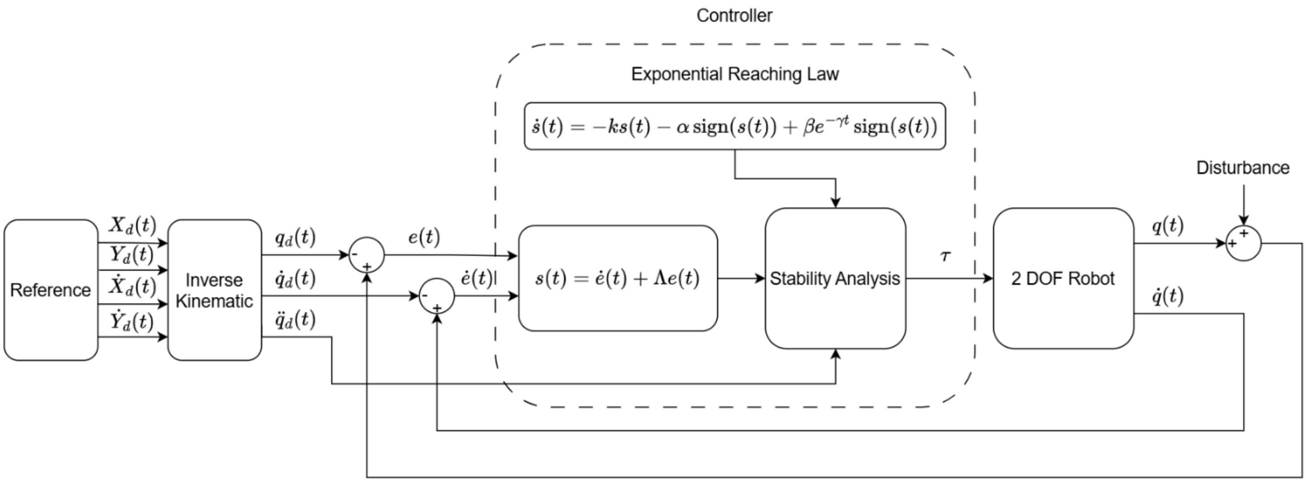

Figure 2. Control structure.

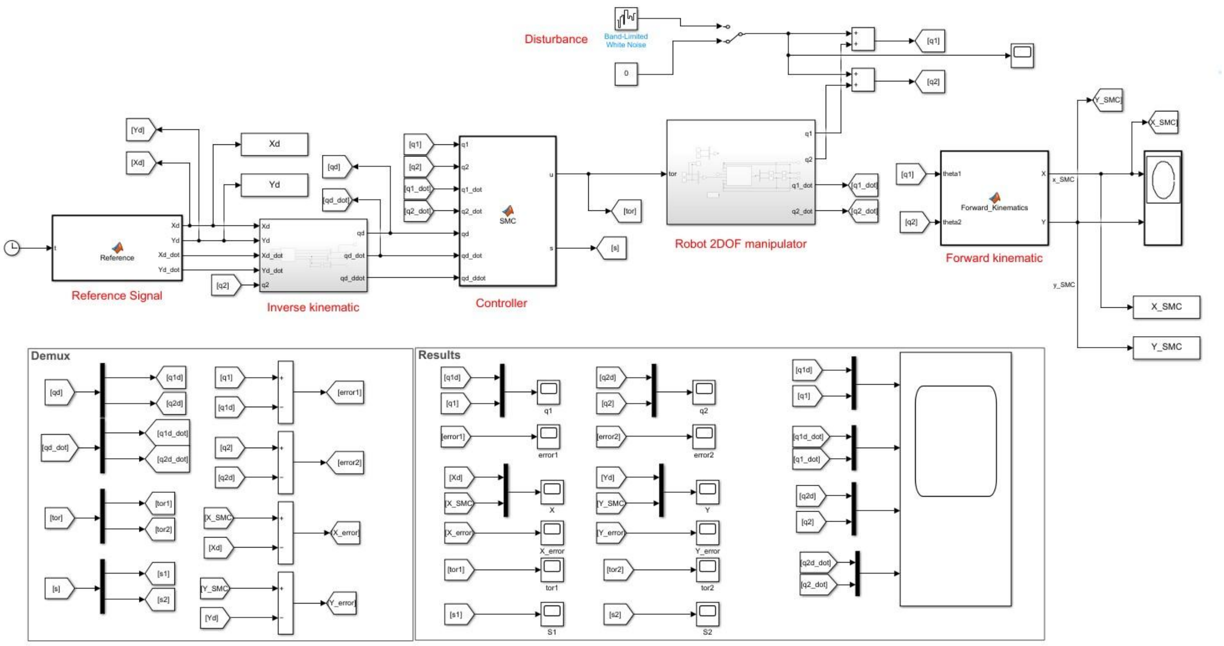

Figure 3. Simulink simulation.

The simulation was conducted under three representative scenarios:

- First, the system was tested under nominal conditions, with no external disturbances or parameter variations. This scenario serves as a baseline to evaluate the tracking performance of the controller in an ideal operating environment.
- Second, external disturbances were introduced to evaluate the robustness of the ERL-SMC and its ability to maintain accurate trajectory tracking in the presence of perturbations.
- Third, to evaluate robustness against modeling uncertainties, the masses of both links were increased while keeping the controller unaware of these changes. Specifically, the parameters were set to $\boldsymbol{m_1 = 7\,kg, m_2 = 4\,kg, l_1 = l_2 = 0.3\,m}$. This scenario simulates the presence of unmodeled payloads or inaccurate mass estimations, which are common in practical robotic applications.

The simulation results for all three test scenarios are presented and analyzed in Figures 4 to
.

10. These figures demonstrate the effectiveness of the proposed ERL-SMC controller in terms of joint angle tracking accuracy, disturbance rejection, and robustness against mass variations.

Figures 4 and 5 present the joint angle tracking results for $\boldsymbol{\theta_1}$ and $\boldsymbol{\theta_2}$ under nominal conditions, i.e., in the absence of external disturbances or parameter variations. The reference trajectories (dashed red lines) are compared with the actual joint responses (solid blue lines), clearly demonstrating the high tracking accuracy achieved by the proposed controller.

In Figure 4, the tracking response of $\boldsymbol{\theta_1}$ begins from an initial angle of approximately $\mathbf{1.05}$ radians and rapidly converges to the desired sinusoidal reference trajectory. The proposed controller achieves accurate tracking with minimal overshoot. The peak and minimum values of $\boldsymbol{\theta_1}$ reach approximately $\mathbf{1.94}$ radians and $\mathbf{1.10}$ radians, respectively, both closely matching the reference signal. The transient response is short approximately $\mathbf{1.5}$ seconds after which the trajectory stabilizes with negligible steady-state error

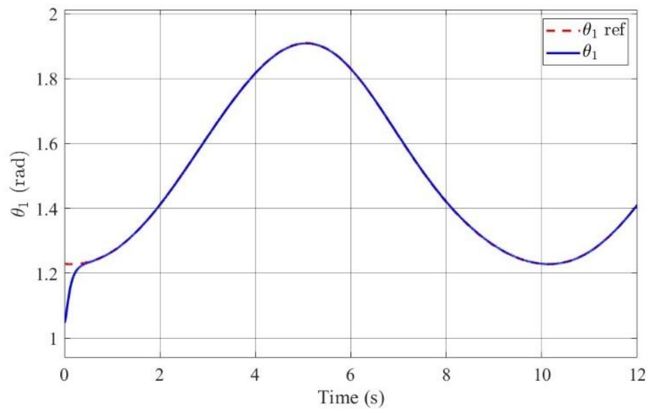

Figure 4. Joint angle tracking result for $\boldsymbol{\theta_1}$ under nominal conditions.

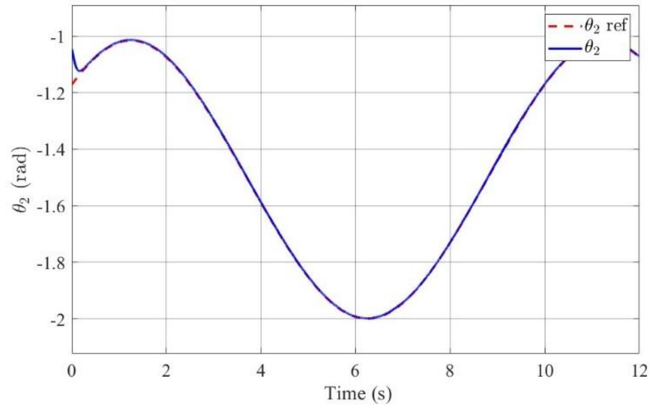

Figure 5. Joint angle tracking result for $\boldsymbol{\theta_2}$ under nominal conditions.

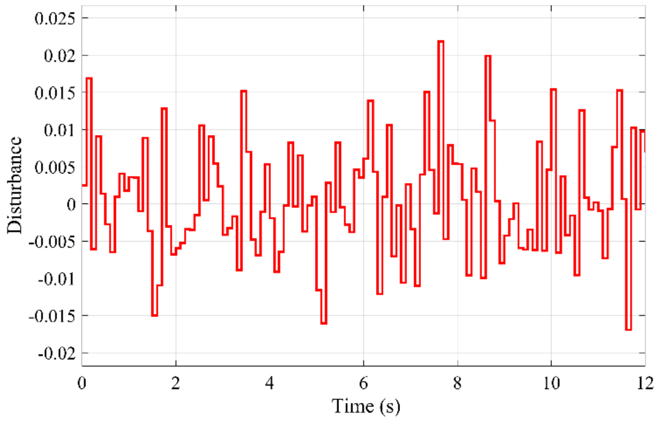

Figure 6. External disturbance.

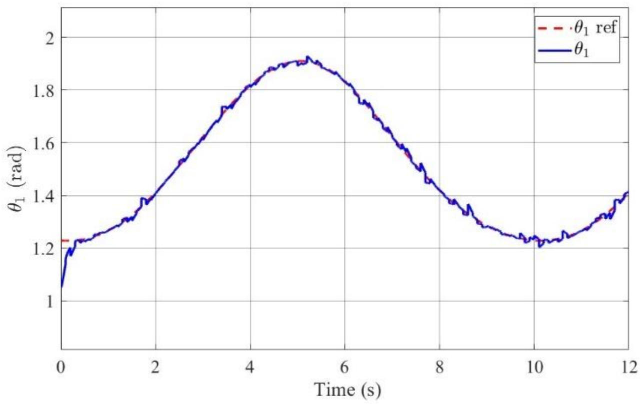

Figure 7. Joint angle tracking for $\boldsymbol{\theta_1}$ under external disturbance.

Figure 5 illustrates the tracking performance of the second joint $\boldsymbol{\theta_2}$. Starting from an initial position of approximately $\mathbf{-1.05}$ radians, $\boldsymbol{\theta_2}$ closely follows the desired periodic trajectory. During its motion, the joint reaches a minimum of approximately $\mathbf{-2.05}$ radians and a maximum of about $\mathbf{-1.05}$ radians. The actual response exhibits excellent agreement with the reference signal, with no observable phase lag or steady-state error.

In this scenario, the actual joint trajectories of the robot closely follow the desired trajectories, highlighting the excellent convergence properties of the proposed controller. The transient phase is brief, and the system rapidly settles into a stable periodic motion that accurately corresponds to the desired circular trajectory in task space. These results confirm that the ERL-SMC provides smooth and precise tracking performance under ideal operating conditions.

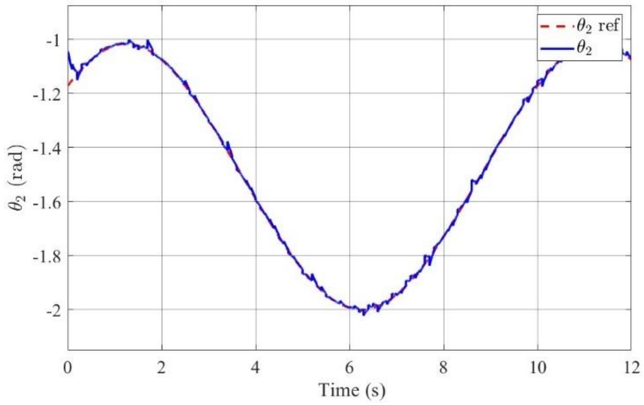

Figure 8. Joint angle tracking for θ_2 under external disturbance.

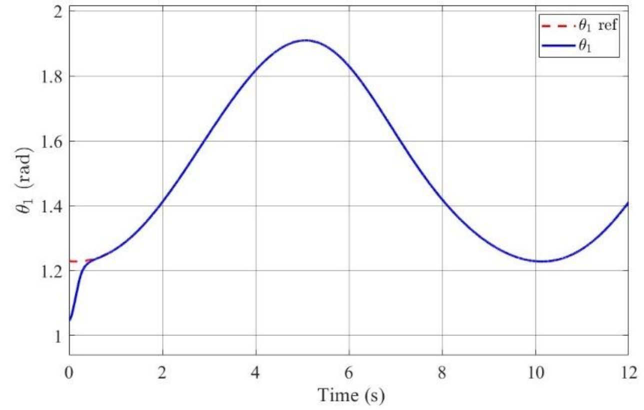

Figure 9. Tracking result for θ_1 under parameter variation (increased mass).

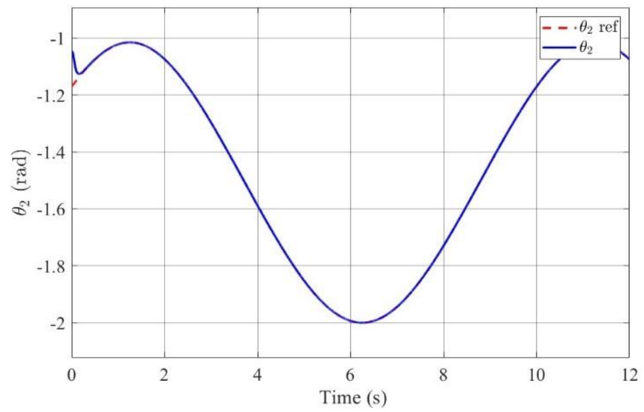

Figure 10. Tracking result for θ_2 under parameter variation (increased mass).

Figures 7 and 8 show the tracking performance of joints θ_1 and θ_2 under the influence of external disturbances (Figure 6) applied during the simulation. In Figure 7, the response of θ_1 remains stable and closely follows the desired trajectory. Small oscillations appear along the actual trajectory. However, these oscillations are bounded and do not significantly degrade the tracking quality. The maximum deviation from the reference remains within ± 0.05 radians, and the overall shape of the trajectory is preserved. This indicates that the exponential reaching law contributes to effective disturbance rejection while maintaining robust convergence. Figure 8 presents the performance of joint θ_2 under similar disturbance conditions. The trajectory exhibits more visible high-frequency ripples compared to the nominal case, particularly near peak positions. However, the main trajectory is still tracked accurately, with minimal phase lag. The controller maintains a tight bound on the tracking error, and the oscillations do not accumulate over time, confirming the inherent robustness of the sliding mode framework.

Despite these perturbations, the controller maintains stable operation and only shows minimal deviations from the reference trajectory. The tracking errors remain bounded, and the system is able to recover quickly, confirming the robustness of the sliding mode controller enhanced with the exponential reaching law. Figures 9 and 10 illustrate the tracking performance of joints $\boldsymbol{\theta_1}$ and $\boldsymbol{\theta_2}$ when the robot operates under parameter variation conditions, specifically with increased link mass. In this scenario, the actual masses of the links were increased over $\mathbf{20}$%, while the controller was still operating based on the original nominal model. This test simulates modeling uncertainties, such as the presence of unknown payloads or parameter estimation errors. As shown in Figure 9, joint $\boldsymbol{\theta_1}$ continues to track the reference trajectory accurately, with only a slight initial deviation during the first few seconds. The trajectory stabilizes quickly and closely follows the sinusoidal reference with minimal steady-state error or phase lag. The smooth convergence of the actual trajectory to the desired path confirms that the proposed ERL-SMC controller is robust against moderate modeling uncertainties. Similarly, Figure 10 shows that the tracking performance of $\boldsymbol{\theta_2}$ remains excellent even with the increased mass. The joint responds smoothly, and the actual trajectory overlaps the reference signal throughout the simulation duration. No significant oscillations, overshoot, or delay are observed. This behavior indicates that the controller maintains high accuracy despite not being retuned for the modified system parameters.

Overall, the simulation results validate that the proposed ERL-SMC control scheme offers excellent performance in terms of fast and accurate convergence in the nominal case, robustness to external disturbances, and strong resilience to modeling uncertainties such as mass variation. Moreover, the exponential reaching law contributes significantly to reducing chattering, leading to smooth control actions and stable joint torques throughout all test scenarios.

5. CONCLUSION

This study proposed an exponential reaching law-based sliding mode control (ERL-SMC) scheme for a two-degrees-of-freedom (2-DoF) planar robotic manipulator. The controller was developed to enhance robustness and mitigate chattering by incorporating an exponentially decaying switching term into the reaching law. Lyapunov-based stability analysis established the global asymptotic convergence of the tracking error. Comprehensive simulation results conducted under nominal conditions, external disturbances, and parametric uncertainties validated the effectiveness of the proposed method in achieving accurate trajectory tracking, rapid convergence, and strong robustness, even in the presence of mass variations and external perturbations.

Future work will involve implementing the proposed controller on a physical robotic platform to validate its effectiveness in real-world environments. Potential extensions include the integration of adaptive or intelligent gain-tuning mechanisms, as well as the application of the control strategy to higher-degree-of-freedom manipulators and cooperative multi-agent systems. Moreover, analyzing energy efficiency and actuator effort under the ERL-SMC framework may offer valuable insights for performance optimization in practical deployments.

REFERENCES

[1] Jin, Y., Li, D., Shi, J., Hao, P., Sun, F., Zhang, J., Fang, B. (2024). Robotgpt: Robot manipulation learning from chatgpt. IEEE Robotics and Automation Letters, 9(3), 2543-2550.

[2] Nguyen, A. T., Dequidt, A., Nguyen, V. A., Vermeiren, L., Dambrine, M. (2021). Fuzzy descriptor tracking control with guaranteed L error bound for robot manipulators. Transactions of the Institute of Measurement and Control, 43(6), 1404-1415.

[3] Han, D., Mulyana, B., Stankovic, V., Cheng, S. (2023). A survey on deep reinforcement learning algorithms for robotic manipulation. Sensors, 23(7), 3762.

[4] Wu, J., Yu, G., Gao, Y., Wang, L. (2018). Mechatronics modeling and vibration analysis of a 2-DOF parallel manipulator in a 5-DOF hybrid machine tool. Mechanism and Machine Theory, 121, 430-445.

[5] Liang, D., Song, Y., Sun, T., Jin, X. (2018). Dynamic modeling and hierarchical compound control of a novel 2-DOF flexible parallel manipulator with multiple actuation modes. Mechanical Systems and Signal Processing, 103, 413-439.

[6] Nguyen, V. A., Vermeiren, L., Dequidt, A., Nguyen, A. T., Dambrine, M., Cung, L. (2018, May). Takagi-Sugeno fuzzy descriptor approach for trajectory control of a 2-DOF serial manipulator. In 2018 13th IEEE Conference on Industrial Electronics and Applications (ICIEA) (pp.1284-1289). IEEE.

[7] Gaidhane, P. J., Nigam, M. J., Kumar, A., Pradhan, P. M. (2019). Design of interval type-2 fuzzy precompensated PID controller applied to twoDOF robotic manipulator with variable payload. ISA transactions, 89, 169-185.

[8] Qin, M., Dian, S., Guo, B., Tao, X., Zhao, T. (2022). Fractional-order SMC controller for mobile robot trajectory tracking under actuator fault. Systems Science Control Engineering, 10(1), 312-324.

[9] Zhu, Q., Huang, D., Yu, B., Ba, K., Kong, X., Wang, S. (2022). An improved method combined SMC and MLESO for impedance control of legged robots' electro-hydraulic servo system. ISA transactions, 130, 598-609.

[10] Wang, X., Wang, D., Du, M., Song, K., Ni, Y., Li, Y. (2023). A two-layer trajectory tracking control scheme of manipulator based on ELM-SMC for autonomous robotic vehicle. IEEE Transactions on Automation Science and Engineering.

[11] Almakki, A., Mazalov, A., Benbouhenni, H., Bizon, N. (2023). Comparison of two fractional-order high-order SMC techniques for DFIGbased wind turbines: Theory and simulation results. ECTI Transactions on Electrical Engineering, Electronics, and Communications, 21(2), 249817-249817.

[12] Srinivasan, S., Arivukkannu, E., Muthiah, R. (2022). A fuzzy sliding mode controller for power quality improvement of solar PV interleaved parallel inverters in a micro-grid. International Journal of Ambient Energy, 43(1), 8386-8399.

[13] Pan, J., Li, W., Zhang, H. (2018). Control algorithms of magnetic suspension systems based on the improved double exponential reaching law of sliding mode control. International Journal of Control, Automation and Systems, 16(6), 2878-2887.

[14] Liu, Y., Wang, Z., Xiong, L., Wang, J., Jiang, X., Bai, G., ... Liu, S. (2018). DFIG wind turbine sliding mode control with exponential reaching law under variable wind speed. International Journal of Electrical Power Energy Systems, 96, 253-260.

BIOGRAPHY:

Van Vuong Dinh He received his B.Eng. degree in Automation Technology from Electric Power University in 2011, and obtained his M.Sc. degree in Control Engineering and Automation from the Military Technical Academy in 2014. He later received his Ph.D. degree in Control Engineering and Automation from Hanoi University of Science and Technology in 2024. He is currently with the Department of Control and Automation at Electric Power University.

His main research interests include robotics and robot control, artificial muscles, and control theory.